

EFFECT OF MICROSTRUCTURE ON TENSILE PROPERTIES OF AUSTENITE-FERRITE WELDED JOINT

Received – Primljeno: 2014-04-01

Accepted – Prihvaćeno: 2014-09-30

Original Scientific Paper – Izvorni znanstveni rad

Complex microstructure of austenite-ferrite welded joint has been investigated, focused on its influence on local tensile properties. Tensile properties (yield strength and hardening coefficient) have been evaluated by using finite element method to simulate the strain distributions obtained experimentally. The three-dimensional model of V-joint specimen has been used with seven different materials, simulating two base metals, the weld metal and two sub-regions of two heat-affected zones - fine grain and coarse grain. In this way local tensile properties of the whole austenite-ferrite welded joint have been evaluated.

Key words: Austenite-ferrite weldment, microstructure, tensile properties, strain chain, strain gages

INTRODUCTION

Structural integrity analysis of welded joints requires knowledge of complex stress and strain distribution in a heterogeneous material, consisting of weld metal (WM), heat-affected-zone (HAZ) and base metal (BM) of different microstructure and mechanical properties [1-8]. This is even more complex problem when two different base metals are welded, like in the case of ferrite-austenite welded joint [9].

Due to very complex microstructure of HAZ and its extremely small size compared to WM and BM, it is not possible to determine the tensile properties of HAZ. This problem is also pronounced if ferrite-austenite welded joint is analysed, because two different HAZ are involved [9]. Therefore, the HAZs tensile properties have to be estimated. In this paper an estimation procedure of the HAZs tensile properties will be presented, based on numerical simulation of the experiment, consisting of strain measurement with strain gages and chains.

MICROSTRUCTURE

The ferrite – austenite welded joint has been made of austenitic steel X6CrNiMo17.12.2 (EN 10088, marked as X6 in this paper), and high strength low alloyed steel NIOVAL 47 (marked as M), by using shielded manual metal arc welding (SMAW) and INOX 29/9 electrode (marked as ASW - all weld metal).

Tensile properties of both steels and electrode all weld metal are listed in Table 1. The chemical composi-

tions of both steels and electrode all weld metal are given elsewhere [9].

Table 1 **Tensile properties of welded joint - reference values**

	M	AWS	X6
Yield Strength $R_{p0.2}$ / MPa	435	545	324
Tensile Strength R_m / MPa	555	755	595
Elongation A_5 / %	25	35	37
Modulus of Elasticity E / GPa	207	193	193

Micrographs of characteristic locations of HAZ of steel M are shown in Figure 1. The HAZ in weld root consists of homogeneous fine-grains ferrite-pearlite microstructure and non-etched WM surface (a), ferrite-pearlite microstructure in the central part (b), coarse grains bainite microstructure close to weld face (c).

Figure 2 shows micrographs showing dendritic structure of WM. Coarse grains with increased contribution of δ ferrite in structure of the last pass are typical for this type of WM.

Micrographs of dissimilar welded joint and microstructures of HAZ fusion region of steel X6 are shown in Figure 3. Structure at fusion line is shown in Figure 3(a), whereas the austenitic microstructure in HAZ in the middle of the sample in Figure 3(b), together with the dark etched WM surface.

Both HAZs comprise fine and coarse grains regions, having significantly different microstructure. In this way austenite-ferrite welded joint has at least seven zones of different properties. Finally, microstructures of both base metals are shown in Figure 4, the base metal M in Figure 4(a), and the base metal X6 in Figure 4(b).

EXPERIMENTAL PROCEDURE

Flat tensile specimens were machined from two base metals and the whole welded joint to determine the

R. Bakić, Tutin High School, Serbia, M. O. Abukresh, A. Sedmak, Faculty of Mechanical Engineering, University of Belgrade, Serbia, I. Samardžić, Faculty of Mechanical Engineering, Slavonski Brod, University of Osijek, Croatia, R. Jovičić, Innovation centre of the Faculty of Mechanical Engineering, Belgrade, Serbia

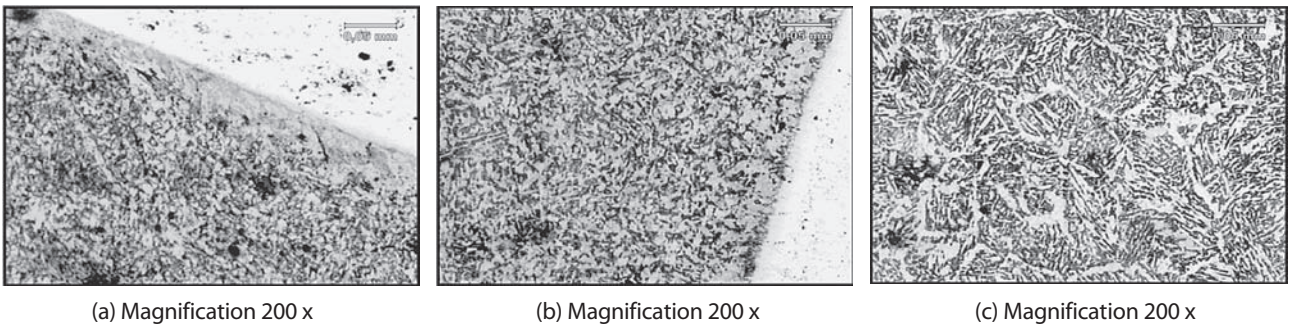


Figure 1 Micrograph of HAZ - base metal M

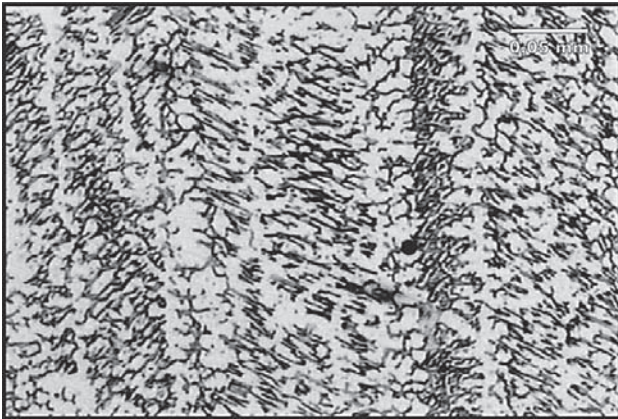
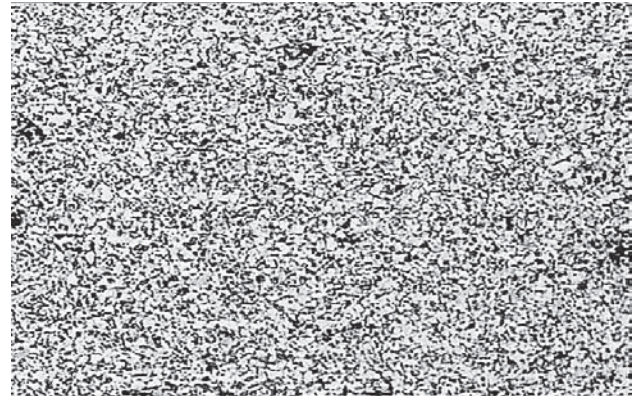
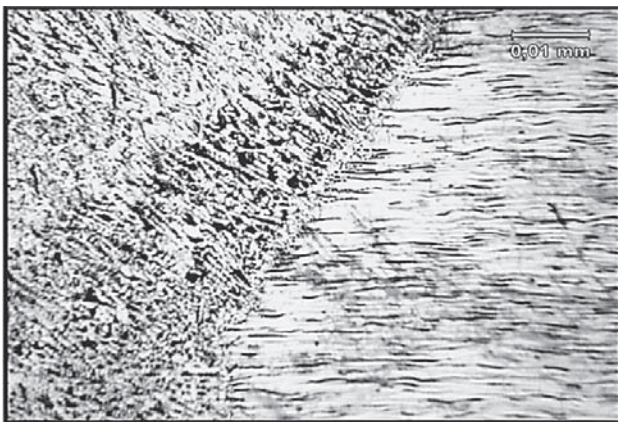


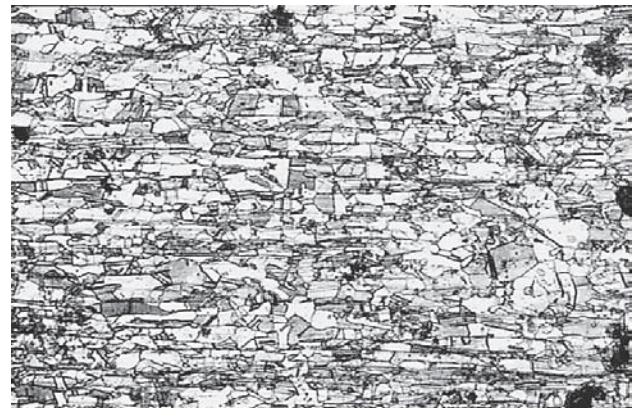
Figure 2 Micrograph of WM Magnification 200 x



(a) Magnification 200 x



(a) Magnification 200 x



(b) Magnification 200 x

Figure 4 Micrograph of base metals, M and X6



(b) Magnification 200 x

Figure 3 Micrograph of HAZ – base metal X6

stress-strain curves. The weld metal itself was tested by using circular cross-section specimen. The results indicate different behaviour of two base metals - continuous curve for steel X6 and the curve with typical yielding behaviour for steel M, as shown in Figure 5(a) and (b), respectively, and explained in more details in [9]. Also, complex behavior of the whole welded joint should be noticed, Figure 5(c), caused by lower value of Yield Strength and higher value of Tensile Strength of the base metal X6, compared to the base metal M.

The modulus of elasticity, yield strength and hardening coefficient are given in Table 2 for both base metals and the weld metal. The hardening coefficient were determined as the ratio of the difference between tensile and yield strength and different ratios of total strain: 1/2

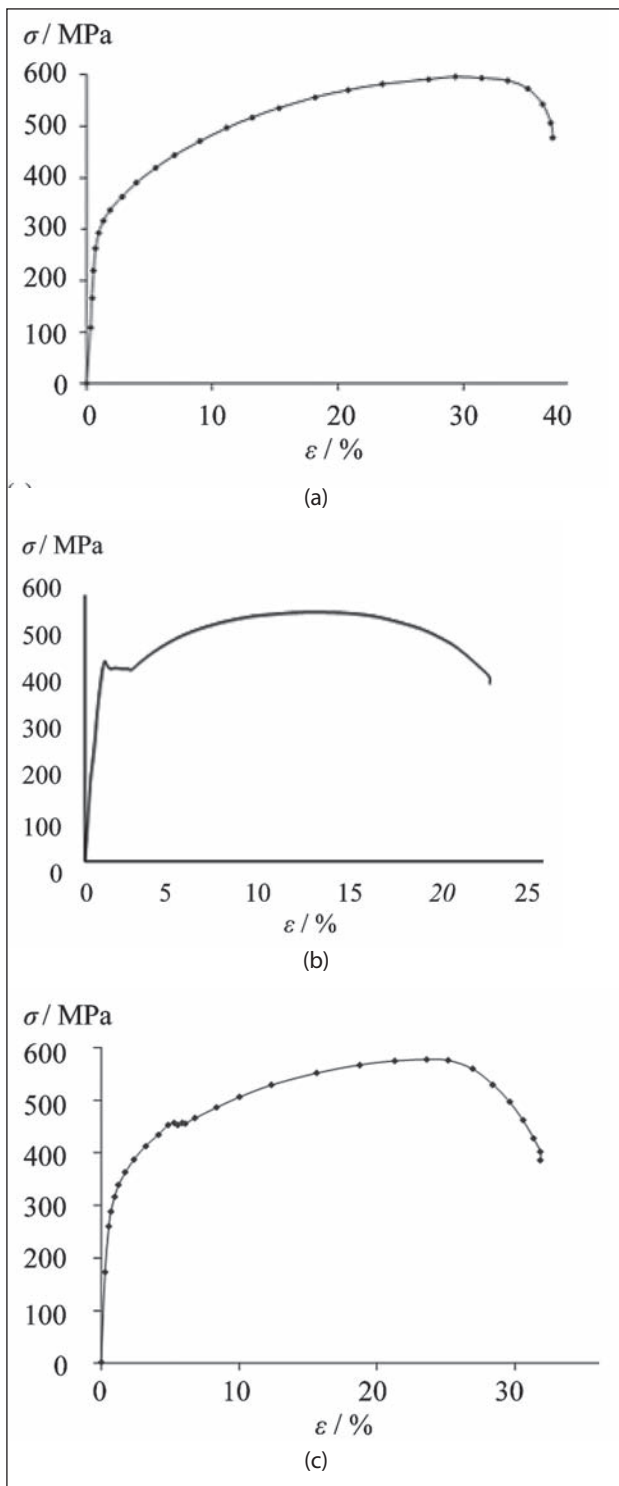


Figure 5 Stress-strain curves for base metals and welded joint as the whole

for steel X6, 2/3 for steel M and 4/7 for weld metal, as explained in [9].

In order to evaluate strain distribution in the welded joint, two tensile panels have been instrumented with strain gages, as shown in Figure 6.

Table 2 Tensile properties - measured

Material	$R_{p0.2}$ / MPa	R_m / MPa	A_5 / %	E / GPa	H' / MPa
Steel X6	335	670	48	193	1400
Steel M	455	616	33	207	730
AWM	545	685	35	193	700

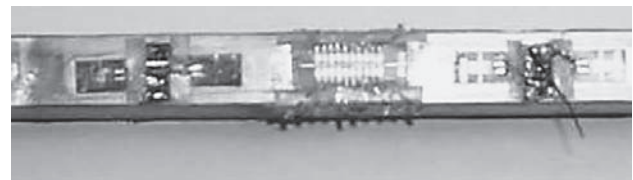


Figure 6 Experimental setup

A total of 12 strain gages and 4 strain chains were used for each tensile panel, positioned at each side of the specimen, Figure 6. Results for average value of measurements at four sides of a specimen are shown in Table 3.

Table 3 Experimental results - average strain values

mat.	2	2	2	2,7	7,6	6,3	3
ave.	11,38	12,18	12,67	11,05	7,75	4,88	2,22
mat.	3	3,5	5,4	4,1	1	1	1
ave.	1,66	1,46	2,67	3,94	5,04	5,98	6,27

Materials are denoted from 1 to 7, as follows:

- 1 and 2 are BM, M and X6, respectively,
- 3 is WM,
- 4 and 5 are CGHAZ and FGHAZ of M,
- 6 and 7 are CGHAZ and FGHAZ of X6.

NUMERICAL SIMULATION

The finite element method has been used to simulate the strain distributions obtained experimentally. The three-dimensional model of V-joint (45°) specimen is shown in Figure 7, with seven different materials indicated by numbers 1-7. The three-dimensional isoparametric finite elements with 20 nodes were used to create a mesh. The maximum remote stress was 425 MPa.

The specimen was modeled with seven different materials, as defined in Table 4 and explained in more details in [9]. Initial values were obtained according to micro-hardness measurement [9].

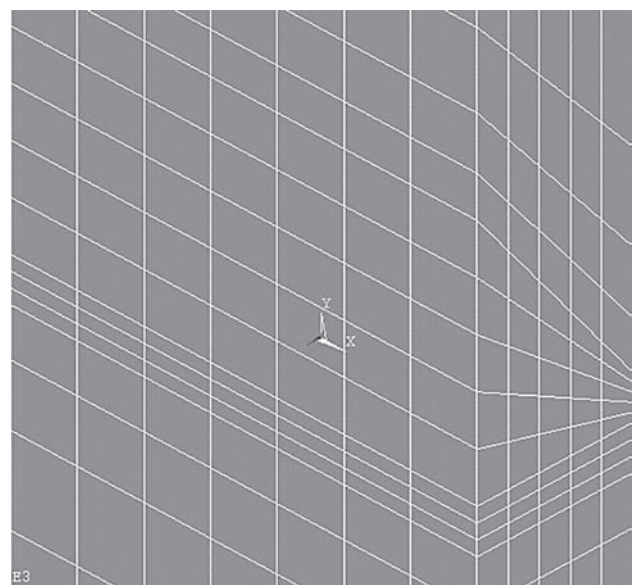


Figure 7 The Finite Element Model with 7 different materials

Tensile properties of both CG HAZ and FG HAZs, needed for the calculation (Yield Strength and hardening coefficient), were varied until numerical strain distributions matched closely enough the experimental ones. Five iterations, i.e. different sets of tensile properties, were used to match the experimental strain distribution, as shown in more details in [9].

The results of this procedure are given in Table 4 for the first and last iteration.

Table 4 Results for the 1st and 5th iteration

	1 st Iteration		5 th Iteration	
	$R_{p0.2}$ / MPa	H' / MPa	$R_{p0.2}$ / MPa	H' / MPa
1 - X6	355	1 400	355	1 400
2 - M	455	730	455	730
3 - WM	545	700	650	400
4 - CGHAZ-f	550	300	550	300
5 - FGHAZ-f	400	1 000	450	1 200
6 - CGHAZ-a	400	400	630	500
7 - FGHAZ-a	300	1 000	400	1 600

RESULTS AND DISCUSSION

Based on the comparison of numerical and experimental results one can see that minimum seven different materials (WM, two BMs, two CGHAZs and two FGHAZs) should be taken into account when austenite-ferrite welded joint is modeled. Since it was not possible to extract tensile specimens from small regions like CGHAZs and FG HAZs, the iteration procedure has been applied, providing reliable results for all 7 different regions. One should notice that not only these two basic tensile properties differ, but the whole tensile behavior as well. It is also to be noted that the austenite BM has the largest strengthening modulus and the smallest yield strength, whereas the WM has the smallest strengthening modulus and the largest yield strength. Finally, one should keep in mind that HAZs in both base metals, being also heterogeneous, should be modeled by taking into account the fine grain and coarse grain regions, at least. Having in mind complexity of the problem analysed in this paper, one should also keep in mind new possibilities for more precise measurement of strains, e.g. Digital Image Correlation (DIC) method, as described in [10].

CONCLUSION

Based on the results presented in this paper, the following conclusions may be drawn:

- Different microstructures in austenite-ferrite welded joint significantly affect its stress-strain behaviour, due to complex material behavior, involving different yield strength and strengthening levels.
- The iterative method for evaluation of elastic-plastic tensile properties of different regions in a welded joint has been used, based on matching of numerical and experimental results.
- The iterative method proved that HAZ has to be modeled with at least two different regions, coarse-grain and fine-grain.

Acknowledgements

The authors acknowledge financial support by the Ministry for education, science and technology development, Republic of Serbia, projects 174004 and 35002.

REFERENCES

- [1] R. Jovičić, A. Sedmak, S. Sedmak, Lj. Milović, K. Jovičić, Leakage of an Austenitic Steel CO₂ Storage Tank, *Structural Integrity and Life*, 12 (2012) 2, 105-108
- [2] R. Jovičić, S. Petronić, S. Sedmak, U. Tatić, K. Jovičić, Integrity Assessment of Tanks with Microcracks in Welded Joints *Structural Integrity and Life*, 13 (2013) 2, 131-136
- [3] B. Petrovski, M. Kocak, S. Sedmak, Fracture Behavior of undermatched weld joint with short surface crack, *GKSS 91/E/93*, 1993
- [4] D. T. Read, Fracture Toughness of Weldments: Elastic-Plastic fracture Analysis, *ASME Conference, MPC-22*, 1984, 75-90
- [5] N. Gubelj, J. Predan, I. Rak, D. Kozak: Integrity assessment of HSLA steel welded joint with mis-matched strength, *Structural Integrity and Life*, 9. (2009) 3, 157-164
- [6] V. Grabulov, I. Blačić, A. Radović, S. Sedmak Toughness and ductility of high strength steels welded joints, *Structural Integrity and Life*, 8 (2008) 3, 181-190
- [7] M. Manjgo, M. Behmen, F. Islamović, Z. Burzić, Behaviour of Cracks in Microalloyed Steel Welded Joint, *Structural Integrity and Life*, 10 (2010) 3, 235-238
- [8] Lj. Milović, T. Vuherer, Z. Radaković, M. Janković, M. Zrilić, D. Daničić, Determination of Fatigue Crack Growth Parameters in Welded Joint of HSLA Steel, *Structural Integrity and Life* 11 (2011) 3, 183-187
- [9] R. Jovičić, A. Sedmak, K. Čolić, M. Milošević, N. Mitrović, Evaluation of the local tensile properties of austenite-ferrite welded joint, *Chemicke Listy*, 105 (2011), 754-757
- [10] J. Lozanović, Application of stereometric strain measurement at macro and micro level, *Structural Integrity and Life*, 7 (2007) 3, 201-208

Note: For English language translation responsible is prof. Martina Šuto, University of Osijek